



## ANALYSIS AND ASSESSMENT OF DAILY AND SEASONAL PHOTOVOLTAIC HEAT ISLAND EFFECT ON SEKBANDEMIRLI RURAL REGION BY LOCAL WEATHER DATA RECORDS

Emre DEMIREZEN<sup>b,d,\*</sup>, Talat OZDEN<sup>c,d,\*\*</sup> and Bulent G. AKINOGLU<sup>a,b,d,\*\*\*</sup>

<sup>a</sup> Middle East Technical University - Physics Department, Ankara, Turkey

<sup>b</sup> Middle East Technical University - Earth System Science Department, Ankara, Turkey

<sup>c</sup> Gumushane University - Department of Electrical and Electronics Engineering, Gumushane, Turkey

<sup>d</sup> ODTÜ Center for Solar Energy Research and Applications (ODTÜ-GÜNAM), Ankara, Turkey

\*demre@metu.edu.tr, ORCID: 0000-0001-8417-104X

\*\*tozden@metu.edu.tr, ORCID: 0000-0002-0781-2904

\*\*\*bulo@metu.edu.tr, ORCID: 0000-0003-1987-6937

(Geliş Tarihi: 22.12.2021, Kabul Tarihi: 19.07.2022)

**Abstract:** Photovoltaic Power Plants have a considerable share among solar energy conversion technologies toward environmentally sustainable and economically feasible electricity production. However, when a rural region's land surface formed by natural soil types is covered by a Photovoltaic Power Plant (PVPP)'s dark-colored solar modules in large numbers, an artificial albedo (reflectivity) change is expected on that surface. Because of the heat exchange between these modules and the air surrounding them due to albedo alteration, the region's natural weather conditions may experience Photovoltaic Heat Island Effect (PVHIE) as a result of external and time-dependent air temperature oscillations caused by the warming-cooling cycles of solar modules. To observe and analyze a possible PVHIE trend, it has been conducting a field study project since October 2017 for a PVPP near the Sekbandemirli rural region in the Kutahya city of Turkey. The weather data, including air temperature and wind (direction and speed) at every 10-minute and hourly intervals, are collected by the three weather monitoring stations installed at the specific locations inside and outside the PVPP field. The plant's hourly average power output and module temperature data can also be monitored. After conducting statistical, correlational, and graphical analyses, the results show some temporal PVHI formations at the PVPP field center daily and on a seasonal basis. The plant center's air temperature tends to be warmer (up to the 6°C difference) during daytimes and colder (up to the (-3)°C difference) during nighttimes.

**Keywords:** Heat island effect, Air temperature, Photovoltaic power plant, Weather station, Wind direction, Wind speed

## YEREL METEOROLOJİK VERİ KAYITLARI İLE SEKBANDEMİRLİ KIRSAL BÖLGESİNDE GÜNLÜK VE MEVSİMSSEL FOTOVOLTAİK ISI ADASININ İNCELENMESİ VE DEĞERLENDİRİLMESİ

**Özet:** Fotovoltaik enerji santralleri, çevresel açıdan sürdürülebilir ve ekonomik olarak uygulanabilir elektrik üretimine yönelik güneş enerjisi dönüşüm teknolojileri arasında önemli bir paya sahiptir. Ancak, kırsal bir bölgenin doğal toprak türlerinin oluşturduğu arazi yüzeyi, bir fotovoltaik enerji santralinin büyük sayılardaki koyu renkli güneş modülleri ile kaplandığında, bu yüzeyde yapay bir albedo (yansıtma) değişimi beklenir. Albedo değişimi nedeniyle bu modüller ve onları çevreleyen hava arasındaki ısı alışverişine ve ısınma-soğuma döngülerine bağlı olarak oluşan harici ve zamana bağlı hava sıcaklığı salınımları sonucunda, bölgenin doğal hava koşulları "Fotovoltaik Isı Adası Etkisi"ne maruz kalabilir. Olası bir fotovoltaik ısı adası etkisi eğilimini gözlemlemek ve analiz etmek için, Türkiye'nin Kütahya ilinin Sekbandemirli kırsal bölgesi yakınındaki bir fotovoltaik enerji santrali için Ekim 2017'den itibaren bir saha çalışması projesi yürütülmektedir. Her 10 dakikalık ve saatlik aralıklarla hava sıcaklığı ve rüzgar (yön ve hız) dahil olmak üzere hava durumu verileri, santral alanının içindeki ve dışındaki belirli konumlara kurulu üç meteorolojik izleme istasyonu tarafından toplanmaktadır. Santralin saatlik ortalama güç çıkışı ve modül sıcaklık verileri de izlenebilmektedir. İstatistiksel, korelasyonel ve grafiksel analizler yapıldıktan sonra sonuçlar, fotovoltaik enerji santrali sahasının merkezinde günlük ve mevsimsel olarak bazı geçici fotovoltaik ısı adası oluşumlarını göstermektedir. Santral merkezinin hava sıcaklığı, gündüzleri daha sıcak (6°C farka kadar) ve geceleri daha soğuk ((-3)°C farka kadar) olma eğilimindedir.

**Anahtar Kelimeler:** Isı adası etkisi, Hava sıcaklığı, Fotovoltaik enerji santrali, Meteorolojik istasyon, Rüzgar yönü, Rüzgar hızı

## NOMENCLATURE

°C	degree Celsius
$\Delta T$	Temperature Difference
ANOVA	One-Way Analysis of Variance
avg	Average
BLUHI	Boundary Layer Urban Heat Island
CLUHI	Canopy Layer Urban Heat Island
HSD	Honest Significant Difference
m/s	meter/second
NE	North East
P	Hourly Average PVPP Power Output
PV	Photovoltaic
PVHI	Photovoltaic Heat Island
PVHIE	Photovoltaic Heat Island Effect
PVPP	Photovoltaic Power Plant
$T_m$	Module Temperature
$T_{m\_avg}$	Hourly Average Module Temperature
$T_{amb\_avg}$	Hourly Average Ambient Temperature
UHI	Urban Heat Island
UHIE	Urban Heat Island Effect
$W/m^2$	Watt/square-meter
$WS_i$	$i^{th}$ number Weather Station ( $i=1,2,3$ )
$WS_{Ti}$	Temperature measured/recorded by $i^{th}$ number weather station
$WS_{Ti\_avg}$	Hourly Average temperature measured/recorded by $i^{th}$ number weather station
$WS_{WDi}$	Wind Direction measured/recorded by $i^{th}$ number weather station
$WS_{WSi}$	Wind Speed measured/recorded by $i^{th}$ number weather station

## INTRODUCTION

Large-scale use of rural land areas requires utility-scale solar energy systems referring to the immense power plants based on Solar Photovoltaic and Concentrated Solar technologies. While the recent R&D efforts improve the efficiency of cells, modules, and other solar energy devices, and solar electricity becomes more affordable, the construction of these plants is also expanded over cultivated/uncultivated or vacant lands. In this expansion process, the influence of microclimatic factors and determining the optimal installation sites should also be considered (e.g., for the "agrivoltaic systems" which meet the energy demand of agricultural production (Adeh et al., 2018; Adeh et al., 2019; Chamara and Beneragama, 2020; Mokarram et al., 2020). Nevertheless, the alteration of PVPP installations in land use brings an environmental problem into the agenda regarding the energy transfer between those land surfaces and the overlying atmosphere. Because of the changes in the balance between the incoming (shortwave) solar and outgoing

(longwave) terrestrial radiation, a possible HIE can be observable in the regions enclosing a solar photovoltaic power plant site.

HIE is usually defined with prefixes, which specify the type/source of the effect, and the most discussed one is Urban Heat Island Effect (UHIE). Including some researches for different world cities and analysis/modeling methods, UHIs have generally been studied according to the artificially-induced air temperature rises caused by the high-density buildings and low-density green spaces, lack of trees and ponds, vehicle traffic and roads, GHG emissions, etc. of metropolitan areas. Deilami et al. (2018) presented a comprehensive systematic review of UHIE methodology and Spatio-temporal factors. Spatial variability is found in Hardin et al. (2018)'s research: The daytime and nighttime temperatures were monitored for four U.S. cities by utilizing weather stations to understand the UHI intensity and regional air temperature variability under the local weather conditions.

Some UHI-related modeling studies are introduced by Dorer et al. (2013); Mirzaei (2015); Xu. et al. (2017). Dorer et al. (2013) examined UHI according to heat exchange and building energy demand depending on urban microclimate and urban fabric design, including city building geometries and street canyons. Mirzaei (2015) categorized 33 UHI studies by considering their purpose, location, methodology, and significant finding. Xu. et al. (2017) simulated high-rise buildings with stack-effect of split-type air-conditioners and the solar radiation-induced thermal environment around these buildings. Dwivedi and Khire (2014) compile UHI measurement methods and techniques in their work.

In the literature, there is also a variety of location-based UHI analyses made, such as for Ankara (Turkey) by Yuksel and Yilmaz (2008); for Istanbul (Turkey) by Kuscu and Sengezer (2012); for Cyprus by Hadjimitsis et al. (2013); for Chicago (U.S.) by Coseo and Larsen (2014); for Adana (Turkey) by Yilmaz (2015); for Nagpur (India) by Kotharkar and Surawar (2016); for Konya (Turkey) by Canan (2017); for Kendari City (Indonesia) by Aris et al. (2019). In these studies, different methodologies were utilized to understand the formation type, intensity, sources, and factors of daily/seasonal urban heat island effect, such as Landsat satellite images, land surface temperature analysis, meteorological weather stations traverse surveying, etc. The high absorptance and low reflectance of incoming solar radiation on the urban fabric during daytime are followed by the high thermal emittance (longwave InfraRed (IR) radiation) of extra heat during nighttime. Thus, daily UHIE (plus seasonally influenced) cycles can be detectable. Table 1 shows the basic features of

the main UHI formations, Atmospheric and Surface. Here, it is essential to note that the atmospheric UHI observations are made for the canopy (CLUHI) and boundary (BLUHI) layers of the atmosphere. At the same time, Surface UHI (SUHI) is linked to the surface temperature changes along with the urban fabric.

**Table 1.** Essential Features of UHI formations. (US EPA (2014); Dwivedi and Khire (2014); Voogt (2008))

Feature	Surface UHI	Atmospheric UHI
Time of day and season	Presence: All times of the day and night Intensity: During the day and in the summer	Presence: Small or absent during the day Intensity: At night, before dawn, and in the winter
Temperature Variation	Day: 10 – 15 °C Night: 5 – 10 °C	Day: -1 – 3 °C Night: 7 – 12 °C
Identification method / instrument	Remote Sensing (3D, 2D, ground): <ul style="list-style-type: none"> <li>Satellites</li> <li>Aircrafts</li> <li>Some ground systems</li> </ul>	Fixed weather monitoring stations: <ul style="list-style-type: none"> <li>Ground-mounted versions for CLUHI</li> <li>Tower-mounted versions for BLUHI</li> </ul> Mobile traverses: <ul style="list-style-type: none"> <li>Automobiles for CLUHI</li> <li>Aircraft for BLUHI</li> </ul> Vertical sensing: <ul style="list-style-type: none"> <li>SODAR (Sonic Detection and Ranging) for BLUHI</li> </ul> Tethered balloons for BLUHI
Depiction	Thermal imaging	Isotherm mapping, Temperature graphs

As a similar and ensuing issue with fewer studies, PVHIE has been discussed in the literature for the last ten years. Nemet (2009) presents a substitution effect between fossil fuels and the two PV installation scenarios in terms of albedo change and radiative forcing. Turney and Fthenakis (2011) and Hernandez et al. (2014) give a place for this drawback of land use within their articles concerning the environmental impacts of utility-scale solar energy. Armstrong et al. (2014), Barron-Gafford et al. (2016), and Barron-Gafford et al. (2019) demonstrated the ground-vegetation-air energy fluxes before- and after the mounting of a PV module. A few studies associate their field data and simulation/modeling works with PVHIE positively and negatively (Millstein and Menon, 2011; Fthenakis and Yu, 2013; Masson et al., 2014). As shown in Figure 1, heat release from a PV module surface depends on three physical processes: Radiation,

convection, and conduction. These processes are linked to several structural module properties such as solar cells' efficiency (commercially % 10-25 in general) and their packing density, electrical operating point, module heat capacity, and anti-reflective coatings (ARCs) as well.

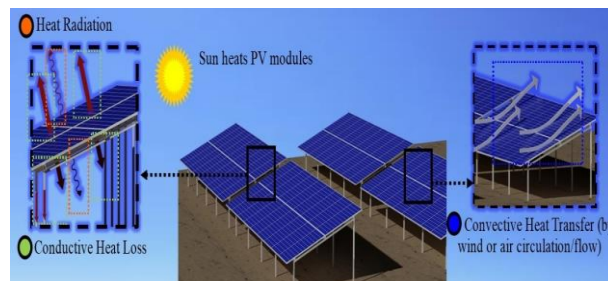


**Figure 1.** Heat Release Processes between PV Module Arrays and Surrounding Air (Demirezen et al., 2022)

In addition to the PVHIE researches above, some studies on thermal modeling (Lobera and Valkealahti, 2013; Siddiqui and Arif, 2013; Tuncel et al., 2018), degradation and reliability (Saadsaoud et al., 2017; Ozden and Akinoglu, 2018), and shading effect (Kiris et al., 2016) analyze PV module temperature and efficiency/performance according to weather/climatic and environmental conditions.

To make the contributions listed below to the previous PVHIE-related studies, it has been conducting the research projects of this field study since October 2017 for a photovoltaic power plant near the Sekbandemirli Village and Rural Region in the Kutahya city of Turkey:

- The first field study of Turkey related to this issue
- A comprehensive PVHIE analysis made by the combination of different methods/techniques (statistical, graphical, and correlational)
- Daily and seasonal assessments made thanks to 2-year field data-collection
- A simulation-based analysis planned for the next stage of the study by using a microclimate and heat island simulation software, ENVI-met
- A beneficial resource for the academicians, researchers, policy-makers, and stakeholders working on PVPP projects

## FIELD STUDY AND METHODOLOGY

Sekbandemirli Village (39.52°N; 29.34°E) is a rural settlement area 16 km away from Tavsanli, one of the Kutahya city's districts in Turkey. As a geographic transition location between Turkey's three regions, its seasonal weather conditions are under Central Anatolia, Aegean, and Marmara climates. Sekbandemirli has mostly mild average temperatures and wind speeds from the category "calm" to "moderate

breeze" (Beaufort scale) throughout the year. The village is surrounded by grasslands and shrublands partly met some steppe fields.

In 2017, Sekbandemirli PVPP (2.5 MW) was constructed on an adjacent uncultivated area (44000 m<sup>2</sup>) of the village with the installations of mono-crystalline and poly-crystalline solar modules having the conversion efficiencies of 18.4 % and 16.6 %, respectively (Figure 3). The front edge of the PVPP's module arrays is 0.5 m above ground, whereas this height is 1.9 m for their rear edge. The solar module tilt angle is 20°.

There are two web interfaces used to monitor the study's field data: The first one, PlantMet (<http://web.plantmet.com.tr>), is an agricultural and meteorological data monitoring system for the measurements of the weather stations WS<sub>1</sub> and WS<sub>2</sub> (every 10-minute and hourly intervals). The second one, SunnyPortal ([www.sunnyportal.com](http://www.sunnyportal.com)), is to track WS<sub>3</sub> (hourly intervals), the PVPP's power output, and the module temperature. Both numerical values and graphical demonstrations can be viewed for the selected dates or date intervals on these interfaces. The methodology diagram of the study is given in Figure 2.

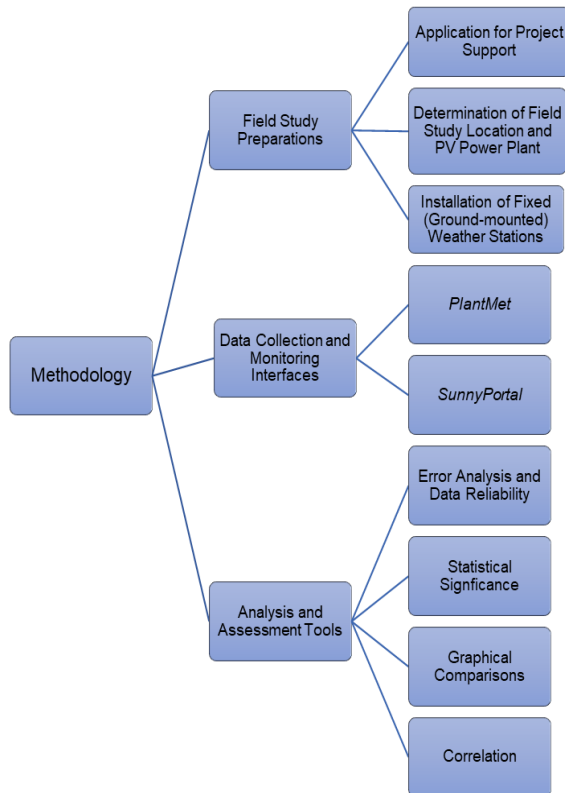
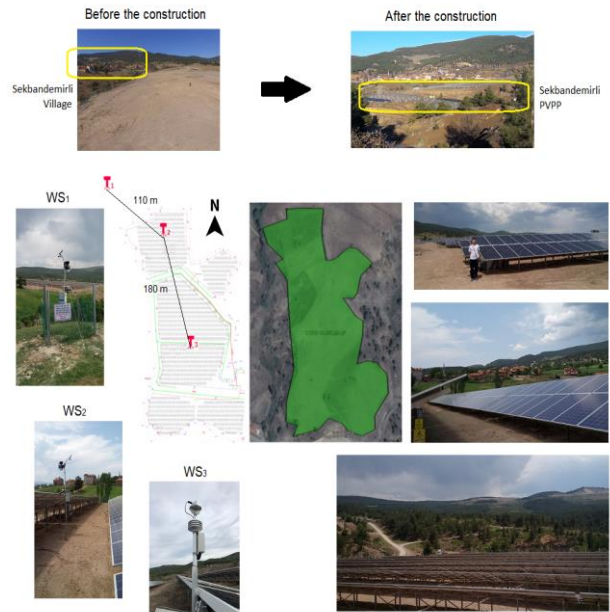


**Figure 2.** Methodology Diagram of the Study

In summary, the PVHI formations in the Canopy Layer were observed in the PVPP field and its close surroundings, and it was planned to use “fixed (ground-mounted) weather monitoring stations” for those

observations. The brand/model and features of these weather stations used are given in the following subsection. In addition, the interfaces where both the meteorological data collected via these weather stations and the PV module temperature and PVPP electrical power output data collected from the PVPP field are monitored on the web will be explained.



(a)



(b)

**Figure 3.** Site Plan (a) and Google Earth View (b) of the Sekbandemirli rural region and PVPP (Red drawings (a) and yellow-colored coordinates (b) show the weather station (WS) locations)

## DATA COLLECTION AND MONITORING

The analysis methods, correlation results, and graphical comparisons of 24-month data collected from November 2018 to October 2020 via the three weather stations (WS<sub>1,2,3</sub>) are explained in the following

sections. This 24-month data includes the main parameters below for PVHIE observation:

- hourly average (hourly averages are calculated from the 10-minute averages between the hours XX:00 – XX:50) air temperature (°C; from outside to the center of the PVPP field as WS<sub>T1,T2,T3</sub> at 2 m above ground)
- photovoltaic module surface temperature (°C; T<sub>m\_avg</sub>)
- average wind speed (m/s; WS<sub>WS1,WS2</sub> at 2.5 m above ground; WS<sub>3</sub> doesn't have wind speed sensor)
- wind direction (degrees; WS<sub>WD1,WD2</sub> at 2.5 m above ground; WS<sub>3</sub> doesn't have wind direction sensor)

The weather measurements below are also collected as supportive data:

- incoming solar radiation (W/m<sup>2</sup>; WS<sub>1</sub>, WS<sub>2</sub>, WS<sub>3</sub>)
- relative humidity (%; WS<sub>RH1</sub>, WS<sub>RH2</sub>; WS<sub>3</sub> doesn't have relative humidity sensor)
- rainfall amount (mm; WS<sub>RA1</sub>, WS<sub>RA2</sub>; WS<sub>3</sub> doesn't have rainfall amount sensor)
- rainfall speed (mm/h; WS<sub>RS1</sub>, WS<sub>RS2</sub>; WS<sub>3</sub> doesn't have rainfall speed sensor)
- barometric pressure (mbar; WS<sub>BP1</sub>, WS<sub>BP2</sub>; WS<sub>3</sub> doesn't have barometric pressure sensor)

Each weather data specified above is grouped as the monthly data sets. Microsoft Office Excel 2019 and its Data Analysis ToolPak were used for the data filtering, the calculations of the results given in the next section, and chart illustrations.

Because WS<sub>3</sub> doesn't have a solar radiation sensor, WS<sub>2</sub>'s incoming solar radiation measurements are required to separate the daytime and nighttime measurements from the daily data inside the PVPP field:

- a daytime value when "not zero"
- a nighttime value when "zero"

The statistical and graphical comparisons, correlation results, and further work will be explained in the following sections.

## RESULTS

### Error Analysis and Data Reliability

The sensor accuracy of weather station measurements (from their technical specification documents) and the confidence intervals calculated from the error analysis of each weather parameter's cumulative data are given in Table 2 (the Microsoft Excel 2019 functions used to calculate the numerical results on the table are specified for each category).

If the confidence level is smaller than sensor accuracy or equals it, this contributes to the usability of the relevant parameter measurements as reliable data. It should also be considered that the weather stations had sometimes failed to send field data (null values) due to some technical problems. As shown in Table 2, the confidence intervals of all the weather parameters are smaller than the accuracy of the WS sensors taking measurements. So, the data reliability is ensured for all the parameters.

**Table 2. Confidence Intervals and Sensor Accuracy**

	WS <sub>T1</sub>	WS <sub>T2</sub>	WS <sub>T3</sub>	T <sub>m_avg</sub>	WS <sub>WS1</sub>	WS <sub>WS2</sub>	WS <sub>WD1</sub>	WS <sub>WD2</sub>
Standard Deviation <sup>a</sup>	8.4	8.5	9.5	14.1	1.1	1.1	98.2	90.8
Standard Error <sup>b</sup>	0.1	0.1	0.1	0.1	0.0	0.0	0.6	0.6
Tcrit <sup>c</sup>	2.0	2.0	2.0	2.0	2.0	2.0	2.0	2.0
Confidence Interval (% 95) <sup>d</sup>	± 0.1°C	± 0.1°C	± 0.2°C	± 0.2°C	0.0 m/s	0.0 m/s	± 1.2°	± 1.1°
Sensor Accuracy <sup>e</sup>	± 0.3°C	± 0.3°C	± 0.3°C	± 0.3°C	± 0.9 m/s	± 0.9 m/s	± 3°	± 3°

a: SUBTOTAL (STDEV.P; Summation of the hourly averages of all the 24 month-data)

b: Standard Deviation / (SQRT (SUBTOTAL (COUNT; Summation of the hourly averages of all the 24 month-data)))

c: TINV(0,05; (SUBTOTAL (COUNT; Summation of the hourly averages of all the 24 month-data) – 1))

d: Tcrit \* Standard Error

e: Technical specification documents of the weather stations:

- WS1 and WS2: Davis / Vantage Pro2™
- WS3: PV-met / 150
- PV module temperature sensor connected to WS3: PV-met / A2101

### Statistical Significance between Weather Stations

In the first publication of the study (Demirezen et al., 2018), two statistical methods were used to compare the first 8-month (10-minute intervals) data sets of WS<sub>1</sub> and WS<sub>2</sub>. The first one, One-Way Analysis of Variance (ANOVA), shows if there are statistically significant differences between the means of three or more independent groups (here, weather stations) or not. Following the results of One-Way ANOVA, the second method is a Post Hoc Test named Tukey's Honest Significant Difference (HSD) particularly shows which of these groups differ from each other. The nearby Tavsanlı WS's data from the Turkish State Meteorological Service (<https://www.mgm.gov.tr>) was provided to meet the requirement of a third WS to perform these methods. Among four weather parameters (air temperature, relative humidity, barometric pressure, and wind speed), the only insignificance between WS<sub>1</sub> and WS<sub>2</sub> was found for air temperature. That is to say; any distinct PVHI formations had not been observed yet around the location of the Sekbandemirli PVPP field surrounding WS<sub>1</sub> or WS<sub>2</sub> (Figure 4).

After the WS<sub>3</sub>'s installation, both these methods were applied to make the comparisons again, and this time, the 24-month (hourly intervals) data sets of three WSs were used. Firstly, the ANOVA results are given in

Table 3. The measurements of three WSs differ significantly on air temperature concerning the two conditions of ANOVA:

$$p\text{-value} = 0.00 < \alpha = 0.05 \text{ (Significance level)} \quad (1)$$

$$F\text{-value} = 47.20 > F_{\text{critical}} = 3.00$$

**Table 3. One-Way ANOVA Results**

Groups	Data Count	Sum	Average (avg)	Variance
WS <sub>1</sub>	16524	221030.80	13.4	76.89
WS <sub>2</sub>	16899	223615.85	13.2	78.08
WS <sub>3</sub>	14210	201377.55	14.2	90.60

Source of Variation	Sum of Squares (S.S.)	Degrees of Freedom (df)	Mean Square (M.S.)	F-value	Fcritical	p-value
Between Groups	7683.87	2	3841.93	47.20	3.00	0.00
Within Groups	3877165.28	47630	81.40			
Total	3884849.14	47632				

The parameters below are used to find the HSD value (Equation (3)) and which of the weather stations differ from each other by Tukey's HSD test:

- MS<sub>within</sub> (from Table 3);
- n (data number for the station having fewer measurements than the other two from Table 3);
- q (from Table 4) values

**Table 4. Q Scores for Tukey's Method**

(k: number of independent groups; df (within): degrees of freedom; α: significance level (0,05))

k	2	3	4	5	6	7	8	9	10
1	18.0	27.0	32.8	37.1	40.4	43.1	45.4	47.4	49.1
2	6.08	8.33	9.80	10.88	11.73	12.43	13.03	13.54	13.99
3	4.50	5.91	6.82	7.50	8.04	8.48	8.85	9.18	9.46
4	3.93	5.04	5.76	6.29	6.71	7.05	7.35	7.60	7.83
5	3.64	4.60	5.22	5.67	6.03	6.33	6.58	6.80	6.99
6	3.46	4.34	4.90	5.30	5.63	5.90	6.12	6.32	6.49
7	3.34	4.16	4.68	5.06	5.36	5.61	5.82	6.00	6.16
8	3.26	4.04	4.53	4.89	5.17	5.40	5.60	5.77	5.92
9	3.20	3.95	4.41	4.76	5.02	5.24	5.43	5.59	5.74
10	3.15	3.88	4.33	4.65	4.91	5.12	5.30	5.46	5.60
11	3.11	3.82	4.26	4.57	4.82	5.03	5.20	5.35	5.49
12	3.08	3.77	4.20	4.51	4.75	4.95	5.12	5.27	5.39
13	3.06	3.73	4.15	4.45	4.69	4.88	5.05	5.19	5.32
14	3.03	3.70	4.11	4.41	4.64	4.83	4.99	5.13	5.25
15	3.01	3.67	4.08	4.37	4.59	4.78	4.94	5.08	5.20
16	3.00	3.65	4.05	4.33	4.56	4.74	4.90	5.03	5.15
17	2.98	3.63	4.02	4.30	4.52	4.70	4.86	4.99	5.11
18	2.97	3.61	4.00	4.28	4.49	4.67	4.82	4.96	5.07
19	2.96	3.59	3.98	4.25	4.47	4.65	4.79	4.92	5.04
20	2.95	3.58	3.96	4.23	4.45	4.62	4.77	4.90	5.01
24	2.92	3.53	3.90	4.17	4.37	4.54	4.68	4.81	4.92
30	2.89	3.49	3.85	4.10	4.30	4.46	4.60	4.72	4.82
40	2.86	3.44	3.79	4.04	4.23	4.39	4.52	4.63	4.73
60	2.83	3.40	3.74	3.98	4.16	4.31	4.44	4.55	4.65
120	2.80	3.36	3.68	3.92	4.10	4.24	4.36	4.47	4.56
∞	2.77	3.31	3.63	3.86	4.03	4.17	4.29	4.39	4.47

If the differences (absolute values) between the averages (Table 3) are bigger than the HSD value, the air temperature measurements of those two weather stations are significantly different from each other. As a result of the comparisons in the equations (4,5,6), the PVPP field's center might be a possible PVHIE source.

$$HSD = q \sqrt{(MS_{\text{within}}/n)} = 3.31 \sqrt{(81,40/14210)} = 0.3 \quad (3)$$

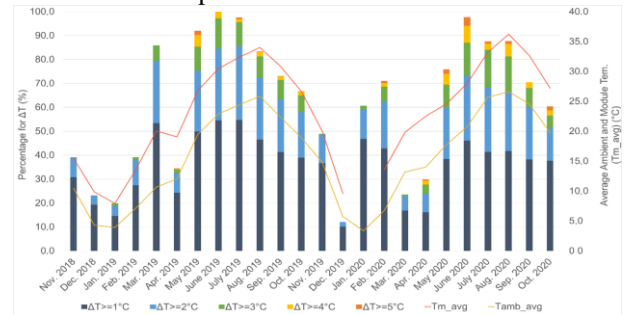
$$WS_{T2\_avg} - WS_{T1\_avg} = 0.2 < 0.3 \text{ (Not signif. diff.)} \quad (4)$$

$$WS_{T1\_avg} - WS_{T3\_avg} = 0.8 > 0.3 \text{ (Signif. different)} \quad (5)$$

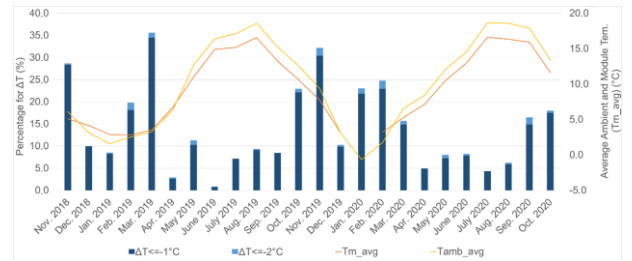
$$WS_{T2\_avg} - WS_{T3\_avg} = 0.9 > 0.3 \text{ (Signif. different)} \quad (6)$$

### Graphical Comparisons

In the previous section, the occurrence of some temporal PVHIs caused by the PVPP is inferred regarding the WS<sub>3</sub>'s data and statistical analyses. This inference is supported by the graphical comparisons of daytime (Figure 4a) and nighttime (Figure 4b) air temperature differences with quantitative data presented below. Among all the 24-month collected data, ΔT percentages correspond to the distribution of ΔT values bigger than 1°C or smaller than -1°C. The T<sub>m\_avg</sub> (hourly average module temperature) and T<sub>amb\_avg</sub> (hourly average air (ambient) temperature) curves were added to the comparisons.



(a)



(b)

**Figure 4. Monthly ΔT Percentages for Daytimes (a) and Nighttimes (b) with T<sub>m\_avg</sub> and T<sub>amb\_avg</sub> curves**

In the daytimes of each of the 24 months, PVHIE can be more or less observable at the PVPP field center, where up to 6°C higher air temperatures were found in Figure 4a. The T<sub>m\_avg</sub> and T<sub>amb\_avg</sub> curves also have a strong relationship with the PVHI formations. Because the T<sub>m\_avg</sub> curve always shows a trendline in the upper position of the T<sub>amb\_avg</sub> curve along the 24 months, the heat exchange (Figure 1) from the solar modules to the overlying atmosphere causes these daytime seasonal positive formations, and they can be observable. Besides, a negative but less effective PVHIE with up to 3°C air temperature differences (WS<sub>T1</sub> > WS<sub>T3</sub>) is more prominent in autumn and winter nights and less detectable in spring and summer nights (Figure 4b) due to the cooling process of the PV modules. Although the T<sub>m\_avg</sub> curve is above the T<sub>amb\_avg</sub> curve along all the seasons except winter, a distinct relation can't be

defined for the nighttime exchanges between each other and this negative PVHIE. The trend curves of monthly maximum daytime (Figure 5a) and minimum nighttime (Figure 5b) air temperatures measured by the WSs support the daily and seasonal PVHIE findings above.

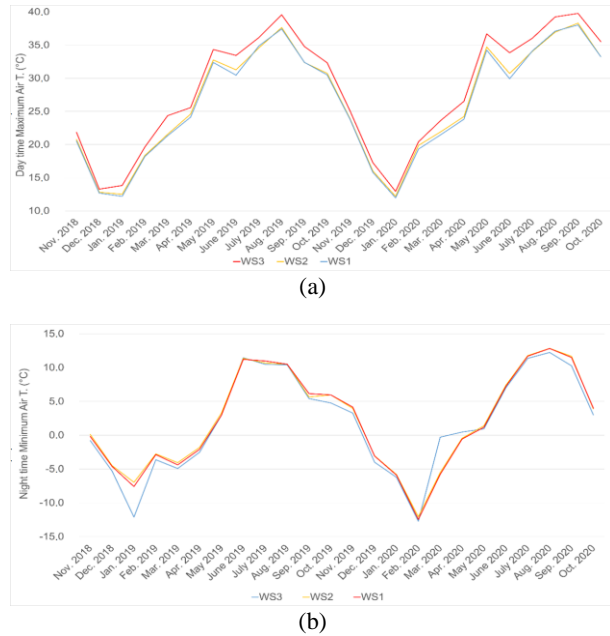


**Figure 5.** Monthly Daytime Maximum (a) and Nighttime Minimum (b) Air Temperature Changes

A graphical illustration of the Sekbandemirli rural region and the measured air temperatures on weather station locations for a day hour of November 2019 and a night hour of August 2019 are given in Figure 6. a PVHI occurrence can be understood towards the field center on November 24 at noon (Figure 6a). An inverse effect resulting in a colder PVPP field center on August 13 at 02:00 is illustrated, too (Figure 6b).

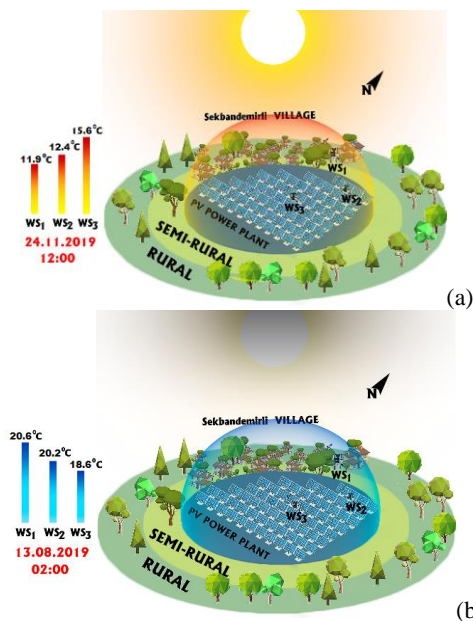


**Figure 6.** PVHI occurrences on a 2019 November day (a) and a 2019 August night (b) in Sekbandemirli Region

## Correlation Results

**Table 5.** Pearson (a) and Spearman (b) Correlation Results for  $\Delta T-T_{m\_avg}$  and  $\Delta T-P$  (closer to +1, the stronger positive linear relationship; closer to -1, the stronger negative linear relationship) (The correlation coefficients couldn't be given for Jan. 2020 due to a technical problem for the  $T_{m\_avg}$  data records)

	$\Delta T-T_{m\_avg}$		$\Delta T-P$		$\Delta T-T_{m\_avg}$		$\Delta T-P$
	Day	Night			Day	Night	
Nov. 2018	0.82	0.11	0.88	Nov. 2019	0.81	-0.11	0.88
Dec. 2018	0.79	-0.04	0.86	Dec. 2019	0.64	-0.04	0.67
Jan. 2019	0.67	0.21	0.62	Jan. 2020	n/a	n/a	0.76
Feb. 2019	0.67	-0.17	0.70	Feb. 2020	0.56	0.21	0.50
March 2019	0.72	0.03	0.69	March 2020	0.75	-0.28	0.79
April 2019	0.48	0.37	0.31	April 2020	0.58	0.59	0.38
May 2019	0.52	0.44	0.34	May 2020	0.49	0.40	0.31
June 2019	0.61	0.54	0.40	June 2020	0.55	0.69	0.33
July 2019	0.55	0.71	0.35	July 2020	0.51	0.70	0.25
Aug. 2019	0.55	0.65	0.32	Aug. 2020	0.51	0.83	0.24
Sept. 2019	0.58	0.68	0.31	Sept. 2020	0.54	0.71	0.32
Oct. 2019	0.57	0.63	0.33	Oct. 2020	0.53	0.57	0.32

(a)

	$\Delta T-T_{m\_avg}$		$\Delta T-P$		$\Delta T-T_{m\_avg}$		$\Delta T-P$
	Day	Night			Day	Night	
Nov. 2018	0.78	0.10	0.91	Nov. 2019	0.82	-0.06	0.91
Dec. 2018	0.73	-0.05	0.86	Dec. 2019	0.70	0.07	0.81
Jan. 2019	0.49	0.13	0.65	Jan. 2020	n/a	n/a	0.78
Feb. 2019	0.69	-0.24	0.76	Feb. 2020	0.52	0.14	0.50
March 2019	0.74	0.07	0.72	March 2020	0.76	-0.29	0.85
April 2019	0.60	0.13	0.46	April 2020	0.66	0.52	0.47
May 2019	0.61	0.36	0.44	May 2020	0.59	0.25	0.47
June 2019	0.65	0.41	0.49	June 2020	0.64	0.56	0.47
July 2019	0.54	0.60	0.38	July 2020	0.52	0.63	0.27
Aug. 2019	0.51	0.58	0.31	Aug. 2020	0.48	0.73	0.24
Sept. 2019	0.57	0.62	0.34	Sept. 2020	0.54	0.62	0.37
Oct. 2019	0.58	0.61	0.38	Oct. 2020	0.58	0.41	0.47

(b)

In terms of linear (Table 5a) and monotonic (Table 5b) relation strength between the air temperature difference  $\Delta T$  ( $WS_{T3}-WS_{T1}$ ), hourly average PVPP power output (P), and hourly average module temperature ( $T_{m\_avg}$ ); Pearson and Spearman correlation coefficients were calculated for daytimes and nighttimes between November 2018 and October 2020. Here,  $\Delta T$  is introduced as the primary indicator of a PVHI.

### Local Winds and PVHIE

Utilizing the 10-minute average wind speed and direction data of WS<sub>2</sub>'s measurements from October 2017 to August 2020, the wind roses for the Sekbandemirli PVPP field were depicted in Figure 7a, considering the maximum speed (up to 8 m/s) and prevailing speed intervals (0-2 and 2-8 m/s) of the region's local winds. They show that the prevailing winds over the PVPP field blow from the North-East (NE) between the speed intervals as follows (according to the Beaufort scale): 0-2 m/s: from "calm air" to "light breeze", 2-8 m/s: from "light breeze" to "moderate breeze".

To understand if these prevailing winds interact with the PVPP's South-facing modules (Figure 7b) and alter the daytime positive PVHIE trend, Figure 8 shows the daytime  $\Delta T$  results associated with the daytime wind direction data (24-month), and the correlation coefficients between the hourly average wind speed measurements and  $\Delta T$  are given in Table 6.

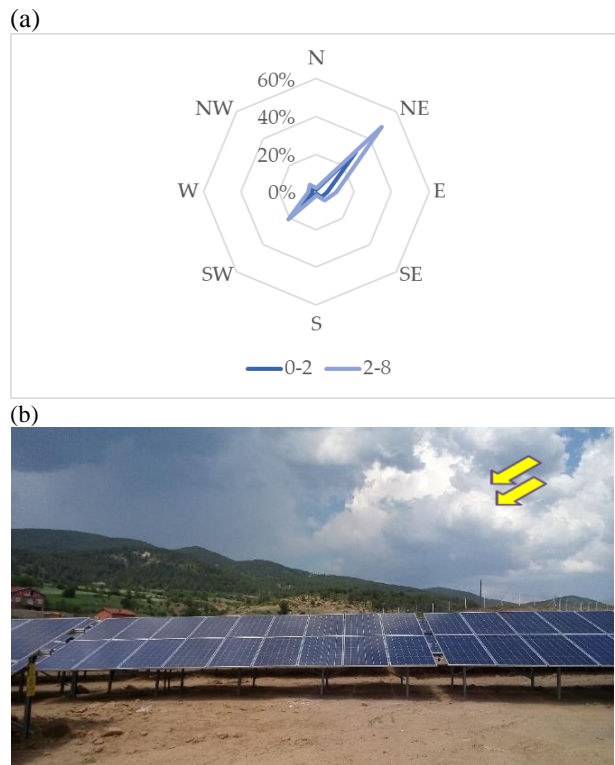


**Figure 7.** Sekbandemirli Region's Wind Rose (a) and Sekbandemirli PVPP's South-Facing Solar Modules (b) (Yellow arrows show the prevailing wind direction as NE)

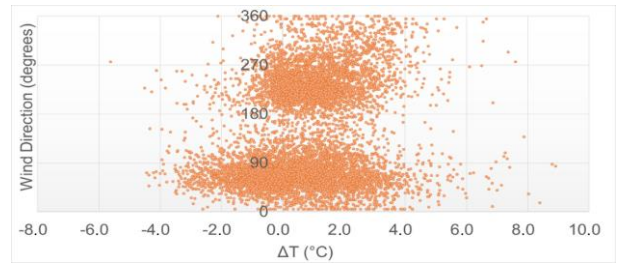


**Figure 8.**  $\Delta T$  associated with Wind Direction data (24-month)

**Table 6.** Pearson (a) and Spearman (b) Correlation Results for  $\Delta T$  - Hourly Average Wind Speed (closer to +1, the stronger positive linear relationship; closer to -1, the stronger negative linear relationship) (The correlation coefficients couldn't be given for Jan. 2020 due to a technical problem for the  $T_{m\_avg}$  data records)

	$\Delta T$ -WS <sub>2</sub> -HAWs		$\Delta T$ -WS <sub>2</sub> -HAWs	
	Day		Day	
Nov. 2018	0.03	Nov. 2019	0.02	
Dec. 2018	0.06	Dec. 2019	-0.18	
Jan. 2019	0.12	Jan. 2020	0.13	
Feb. 2019	-0.06	Feb. 2020	-0.09	
Mar. 2019	-0.04	Mar. 2020	-0.10	
April 2019	0.29	April 2020	0.03	
May 2019	0.12	May 2020	0.00	
June 2019	0.37	June 2020	0.21	
July 2019	0.34	July 2020	0.22	
Aug. 2019	0.27	Aug. 2020	0.25	
Sept. 2019	0.12	Sept. 2020	0.25	
Oct. 2019	-0.18	Oct. 2020	-0.09	

(a)

	$\Delta T$ -WS <sub>2</sub> -HAWs		$\Delta T$ -WS <sub>2</sub> -HAWs	
	Day		Day	
Nov. 2018	0.09	Nov. 2019	0.03	
Dec. 2018	0.07	Dec. 2019	-0.21	
Jan. 2019	0.17	Jan. 2020	0.15	
Feb. 2019	0.00	Feb. 2020	-0.01	
Mar. 2019	-0.06	Mar. 2020	-0.08	
April 2019	0.35	April 2020	0.05	
May 2019	0.15	May 2020	0.02	
June 2019	0.41	June 2020	0.25	
July 2019	0.34	July 2020	0.18	
Aug. 2019	0.27	Aug. 2020	0.24	
Sept. 2019	0.09	Sept. 2020	0.27	
Oct. 2019	-0.16	Oct. 2020	-0.07	

(b)

### DISCUSSION

As seen from the Sekbandemirli Site Plan (Figure 3), by comparing the northern sub-field (WS<sub>2</sub>'s location) and the North-East part outside the PVPP field (WS<sub>1</sub>'s location), the PV module arrays are denser at the center of the PVPP field center where WS<sub>3</sub> is installed. As a result, stronger heat dissipation and interaction between the PV modules and their close/surrounding environment might occur at the field center. Thus, significant air temperature differences between WS<sub>T3</sub> and the other weather stations are detectable (see the "Statistical Significance between Weather Stations" section). Thus, the center of the PVPP field and the PV module arrays here might be a possible heat island source.

As given in the graphical comparisons of the study, the inferences from Figures 4a and 4b are made as follows:

- Figure 4a shows that the overall percentage of positive PVHI formation numbers at the field center gets higher during daytime in the summer months by varying between 0-3°C for 24 months (up to 6°C for some formation intensities). The term “positive” indicates that the PVPP field center is warmer than outside the field. The  $T_{amb\_avg}$  and  $T_{m\_avg}$  curves are directly proportional to the heights of the columns over 24 months. The PV module arrays warm faster than the air surrounding them, so the  $T_{m\_avg}$  curve is at an upper position. When the distance between these curves increases in the summer months, the daytime positive PVHI formations are stronger. Figure 5a, the monthly daytime maximum air temperature changes measured by the weather stations, supports these findings when the WS curves are compared.

- As shown in Figure 4b, the overall percentage of negative PVHI formation numbers at the field center gets higher towards the autumn and winter months by varying between 0-3°C for 24 months. The term “negative” indicates that the PVPP field center is colder than outside the field. The  $T_{amb\_avg}$  and  $T_{m\_avg}$  curves are inversely proportional to the heights of the columns. The PV module arrays cool faster than the air surrounding them on spring and summer nights inferred from the figure; the  $T_{m\_avg}$  curve is at a lower position. In the winter months, the air in the Sekbandemirli region cools faster than the PV module arrays. Therefore,  $T_{m\_avg}$  is at an upper position during these months. In Figure 4b, there is not a significant relationship between the curves and PVHI formation intensity (percentage columns). As a supportive graph for Figure 4b, the monthly nighttime minimum air temperature changes measured by the weather stations are given in Figure 5b.  $WS_3$  recorded mostly lower temperatures than  $WS_1$  and  $WS_2$ .

The study’s correlation results (Pearson and Spearman) are shown in Table 5a and 5b. During daytimes, the relation strength between  $\Delta T$  (PVHI formation intensity) and  $T_{m\_avg}$  tends to be getting weaker from autumn-winter to summer months, getting stronger from summer to winter months.  $\Delta T$  and  $P$  also have similar correlations. Conversely, between these seasons, the  $\Delta T$ - $T_{m\_avg}$  relation strength follows an inverse trend for nighttimes. Because of no electricity production during nighttimes, Table 5a and 5b do not include a nighttime  $\Delta T$ - $P$  correlation column.

In Figure 8, the PVHI formations are apparent with more data points when the wind blows from the directions between 0-90 and 180-270 degrees. Because the prevailing wind direction as NE (45 degrees) has many data points to indicate a PVHI occurrence in Figure 8, it can be concluded that their blowing angle is not convenient to reduce the positive PVHIE at the PVPP’s field center. These local, prevailing winds mostly blow towards the upper right corner of the PV

modules, not their surface, where a natural cooling effect can be provided). Although a slight increase in the correlation strength is observed during the summer months, the inconvenience explained above can also be mentioned by presenting the low or small correlation coefficients between the hourly average wind speed measurements and  $\Delta T$  for most of the year (Table 6).

As for the third stage, it is planned to support the study with a microclimate and heat island simulation software, *ENVI-met* (<https://www.envi-met.com>) (Huttner, 2012; Ambrosini et al., 2014; Sodoudi et al., 2014), which provides a detailed simulation work/analysis by considering measured weather parameters and land cover change on a geographical location. Thus, this extra analysis will develop the current methodology and findings and contribute to the related studies on PVHIE.

## CONCLUSIONS

The ground-based PVPP installations alter land surface albedo (reflectivity) due to their dark-colored solar PV modules (and their heat radiation while operating), and thus, Photovoltaic Heat Island (PVHI) formations might be observable as an atmospheric environmental impact. Although Urban Heat Island Effect is commonly and comprehensively studied in the literature, fewer studies investigate this effect caused by PVPPs. This paper presents our project’s two consecutive stages showing the progressive structure of its findings.

Following the error analysis for data reliability and the statistical analysis for measurement significance, 25-month data of the second stage show daily (day-night) PVHIs occurring at the PVPP’s center with up to 6°C higher air temperatures than the ones measured outside the PVPP field for daytimes. Some inverse (negative) but less-effective PV heat islands are also formed with up to 3°C higher air temperatures outside the field during nighttimes. Monthly maximum air temperatures for daytimes and monthly minimum air temperatures for nighttimes support these results. A graphical illustration of the Sekbandemirli rural region and the measured air temperatures on the weather station locations for a day hour of November 2019 and a night hour of August 2019 is also given in the Results section.

These PVHI formations have specific formation frequencies on a monthly (seasonal) basis. Although solar PV module temperature and power output can be mentioned as the essential determinants or indicators for PVHIE, their correlation weakens from winter to summer and strengthens from summer to winter for daytimes; and vice versa for nighttimes. Simultaneous monitoring of solar module and air (ambient) temperatures should be considered to understand the

PVHI formation mechanism by radiative and convective heat transfer (Figure 1). It should also be noted that the PV module types, which are commercially preferable for land/ground-based PVPP installations, have low heat capacity/high emissivity values taking a significant role in these formations.

As for geographical location choice and sunshine duration analysis, it is also important to investigate a PVPP field's local wind speed and direction before PV module placement and orientation. Wind has capable of reducing HIE by natural convective cooling. On the other hand, having the prevailing wind direction (North-East), the Sekbandemirli PVPP field can't benefit from the region's local winds: They blow onto the solar modules from an inconvenient angle, and thus, they can't cool them during daytimes. Another supportive finding for this inference is that there is a low or no correlation between wind speed and PVHI formation almost all year round.

#### ACKNOWLEDGMENTS

The authors would like to thank Middle East Technical University for financial supports (Project Numbers: BAP-07-02-2017-006 & TEZ-D-105-2020-10169) in the implementation of the study's research projects; Mr. Tolga Eryasar and Mr. Oguz Aydin for their technical assistance; Mr. Ahmet Hamdi Aksoy and Mr. Hakan Akinoglu for their contributions to the study's illustrations.

#### REFERENCES

Ambrosini, D., Galli, G., Mancini, B., Nardi, I., Sfarra, S., 2014, Evaluating Mitigation Effects of Urban Heat Islands in a Historical Small Center with the ENVI-Met® Climate Model. *Sustainability*, 6(10), 7013-7029, doi: 10.3390/su6107013

Aris, A., Syaf, H., Yusuf, D. N., Nurgiantoro, 2019, Analysis of urban heat island intensity using multi temporal landsat data; case study of Kendari City, Indonesia, Paper presented at *Geomatics International Conference 2019*, Surabaya, Indonesia

Armstrong, A., Waldron, S., Whitaker, J., Ostle, N., 2014, Wind farm and solar park effects on plant-soil carbon cycling: Uncertain impacts of changes in ground-level microclimate, *Global Change Biology*, 20(6), 1699-1706. doi: 10.1111/gcb.12437

Barron-Gafford, G. A., Minor, R. L., Allen, N. A., Cronin, A. D., Brooks, A. E., Pavao-Zuckerman, M. A., 2016, The Photovoltaic Heat Island Effect: Larger solar power plants increase local temperatures, *Scientific Reports*, 6(1), doi: 10.1038/srep35070

Barron-Gafford, G. A., Pavao-Zuckerman, M.A., Minor, R.L. et al., 2019, Agrivoltaics provide mutual benefits across the food–energy–water nexus in drylands, *Nat Sustain* 2, 2, 848–855, doi: 10.1038/s41893-019-0364-5

Canan, F., 2017, Kent Geometrisine Bağlı Olarak Kentsel Isı Adası Etkisinin Belirlenmesi: Konya Örneği, *Journal of the Faculty of Engineering and Architecture (Çukurova University)*, 32(3), 69-80, doi: 10.21605/cukurovaummfd.357202

Chamara, R., Beneragama, C., 2020, Agrivoltaic systems and its potential to optimize agricultural land use for energy production in Sri Lanka: A Review, *Journal of Solar Energy Research (JSER)*, 5(2), 417-431, doi: 10.22059/JSER.2020.302720.1154

Coseo, P., Larsen, L., 2014, How factors of land use/land cover, building configuration, and adjacent heat sources and sinks explain Urban Heat Islands in Chicago, *Landscape and Urban Planning*, 125, 117–129, doi: 10.1016/j.landurbplan.2014.02.019

Deilami, K., Kamruzzaman, Md., Liu, Y., 2018, Urban heat island effect: A systematic review of spatio-temporal factors, data, methods, and mitigation measures, *International Journal of Applied Earth Observation and Geoinformation*, 67, 30–42, doi: 10.1016/j.jag.2017.12.009

Demirezen, E., 2022, Monitoring, Analysis, and Simulation of Photovoltaic Heat Island Effect in Turkey: Sekbandemirli Solar Power Plant Field Study, (Doctoral dissertation), Turkey: *Middle East Technical University*.

Demirezen, E., Ozden, T., Akinoglu, B. G. (2018). Impacts of a Photovoltaic Power Plant for Possible Heat Island Effect Paper presented at the *1<sup>st</sup> International Conference on Photovoltaic Science and Technologies (PVCon2018)*, Ankara, Turkey. doi: 10.1109/PVCon.2018.8523937

Dorer, V., Allegrini, J., Orehounig, K., Moonen, P., Upadhyay, G., Kämpf, J., Carmeliet, J., 2013, Modelling the Urban Microclimate and Its Impact on the Energy Demand of Buildings and Building Clusters Paper presented at *13<sup>th</sup> Conference of International Building Performance Simulation Association*, Chambéry, France.

Duman, U., Yilmaz, O., 2008, Ankara Kentinde Kentsel Isı Adası Etkisinin Yaz Aylarında Uzaktan Algılama ve Meteorolojik Gözlemlere Dayalı Olarak Saptanması ve Değerlendirilmesi, *Journal of the Faculty of Engineering and Architecture of Gazi University*, 23(4), 937-952.

- Dwivedi, A., Khire, M. V., 2014, Measurement Technologies for Urban Heat Islands, *International Journal of Emerging Technology and Advanced Engineering*, 4(10), 539-545.
- Fthenakis, V., Yu, Y., 2013, Analysis of the potential for a heat island effect in large solar farms Paper presented at *IEEE 39th Photovoltaic Specialists Conference (PVSC)*, Florida, US.  
doi: 10.1109/PVSC.2013.6745171
- Gokmen, N., Hu, W., Hou, P., Chen, Z., Sera, D., Spataru, S., 2016, Investigation of wind speed cooling effect on PV panels in windy locations, *Renewable Energy*, 90, 283-290, doi: 10.1016/j.renene.2016.01.017
- Hadjimitsis, D., Retalis, A., Michaelides, S., Tymvios, F., Paronis, D., Themistocleous, K., Agapiou, A., 2013, Satellite and Ground Measurements for Studying the Urban Heat Island Effect in Cyprus, *Remote Sensing of Environment - Integrated Approaches*, (pp. 1-24), Cyprus: IntechOpen. doi.org/10.5772/39313
- Hardin, A.W., Liu, Y., Cao, G., Vanos, J. K., 2018, Urban heat island intensity and spatial variability by synoptic weather type in the northeast U.S., *Urban Climate*, 24, 747-762, doi: 10.1016/j.uclim.2017.09.001
- Hassanpour Adeg, E., Selker, J., Higgins, C., 2018, Remarkable agrivoltaic influence on soil moisture, micrometeorology and water-use efficiency, *PLOS ONE*, 13(11), doi: 10.1371/journal.pone.0203256
- Hassanpour Adeg, E., Good, S., Calaf, M., Higgins, C., 2019, Solar PV Power Potential is Greatest Over Croplands, *Scientific Reports*, 9(11442), doi: 10.1038/s41598-019-47803-3
- Hernandez, R. R., Easter, S. B., Murphy-Mariscal, M. L., Maestre, F. T., Tavassoli, M., Allen, E. B., Barrows, C. W., Belnap, J., Ochoa-Hueso, R., Ravi, S., Allen, M. F., 2014, Environmental impacts of utility-scale solar energy, *Renewable and Sustainable Energy Reviews*, 29, 766-779, doi: 10.1016/j.rser.2013.08.041
- Homadi, A., 2016, Effect of Elevation and Wind Direction on Silicon Solar Panel Efficiency, *International Journal of Energy and Power Engineering*, 10, 1205-1212.
- Huttner, S., 2012, Further development and application of the 3D microclimate simulation ENVI-met, (Doctoral dissertation), Germany: *Johannes Gutenberg University of Mainz*.
- Kiris, B., Bingol, O., Senol, R., Altintas, A., 2016, Solar Array System Layout Optimization for Reducing Partial Shading Effect, *Special Issue of the 2<sup>nd</sup> International Conference on Computational and Experimental Science and Engineering (ICCESEN 2015)*, *Acta Physica Polonica A*, 130, doi: 10.12693/APhysPolA.130.55
- Kotharkar, R., Surawar, M., 2016, Land Use, Land Cover, and Population Density Impact on the Formation of Canopy Urban Heat Islands through Traverse Survey in the Nagpur Urban Area, *Journal of Urban Planning and Development*, 142(1), 1-13, doi: 10.1061/(ASCE)UP.1943-5444.0000277
- Lobera, D. T., Valkealahti, S., 2013, Dynamic thermal model of solar PV systems under varying climatic conditions, *Solar Energy*, 93, 183-194, doi: 10.1016/j.solener.2013.03.028
- Masson, V., Bonhomme, M., Salagnac, J. L., Briottet, X., Lemonsu, A., 2014, Solar panels reduce both global warming and urban heat island, *Frontiers in Environmental Science*, 2(14), doi: 10.3389/fenvs.2014.00014
- Millstein, V., Menon, S., 2011, Regional climate consequences of large-scale cool roof and photovoltaic array deployment, *Environmental Research Letters*, 6, doi: 10.1088/1748-9326/6/3/034001
- Mirzaei, P.A., 2015, Recent challenges in modeling of urban heat island, *Sustainable Cities and Society*, 19, 200-206, doi: 10.1016/j.scs.2015.04.001
- Mokarram, M., Mokarram, M., Khosravi, M., Saber, A., Rahideh, A., 2020, Determination of the optimal location for constructing solar photovoltaic farms based on multi-criteria decision system and Dempster-Shafer theory, *Scientific Reports*, 10(8200), doi: 10.1038/s41598-020-65165-z
- Nemet, G. F., 2009, Net Radiative Forcing from Widespread Deployment of Photovoltaics. *Environmental Science & Technology*, 43(6), 2173-2178, doi:10.1021/es801747c
- Ozden, T., Akinoglu, B. G., 2018, Preliminary investigations on two different procedures to calculate the efficiency and performance ratio of PV modules, *International Journal of Environmental Science and Technology*, 16(9), 5171-5176, doi: 10.1007/s13762-018-2003-5
- Saadsaoud, M., Ahmed, A. H., Er, Z., Rouabah, Z., 2017, Experimental Study of Degradation Modes and Their Effects on Reliability of Photovoltaic Modules after 12 Years of Field Operation in the Steppe Region, *Special Issue of the 3<sup>rd</sup> International Conference on Computational and Experimental Science and Engineering (ICCESEN 2016)*, *Acta Physica Polonica A*, 132, doi: 10.12693/APhysPolA.132.930

- Siddiqui, M. U., Arif, A. F. M., 2013, Electrical, thermal and structural performance of a cooled PV module: Transient analysis using a multiphysics model. *Applied Energy*, 112, 300-312, doi: 10.1016/j.apenergy.2013.06.030
- Simsek Kuscü, C., Sengezer, B., 2012, İstanbul Metropolitan Alanında Kentsel Isınmanın Azaltılmasında Yeşil Alanların Önemi, *Megarön*, 7(2), 116-128.
- Smets, A., Narayan, N., 2013, PV Systems: PV Modules II – Temperature dependency of PV output, *DelftX: ET3034TUx Solar Energy*, Delft University of Technology, [https://www.youtube.com/watch?v=v8nbwvC8aBg&t=2s&ab\\_channel=3rabGeeks](https://www.youtube.com/watch?v=v8nbwvC8aBg&t=2s&ab_channel=3rabGeeks)
- Sodoudi, S., Shahmohamadi, P., Vollack, K., Cubasch, U., Che-Ani, A., 2014, Mitigating the Urban Heat Island Effect in Megacity Tehran, *Advances in Meteorology*, 1-19, doi: 10.1155/2014/547974
- Tuncel, B., Ozden, T., Akinoglu, B. G., Balog, R. S., 2018, Thermal Modeling and Verification of PV Module Temperature and Energy Yield Using Outdoor Measurements for Ankara, Turkey Paper presented at the *1<sup>st</sup> International Conference on Photovoltaic Science and Technologies (PVCon2018)*, Ankara, Turkey, doi: 10.1109/PVCon.2018.8523953
- Turney, D., Fthenakis, V., 2011, Environmental impacts from the installation and operation of large-scale solar power plants, *Renewable and Sustainable Energy Reviews*, 15(6), 3261–3270, doi: 10.1016/j.rser.2011.04.023
- Voogt, J., 2008, How Researchers Measure Urban Heat Islands, *US Environmental Protection Agency*, [https://19january2017snapshot.epa.gov/sites/production/files/2014-07/documents/epa\\_how\\_to\\_measure\\_a\\_uhi.pdf](https://19january2017snapshot.epa.gov/sites/production/files/2014-07/documents/epa_how_to_measure_a_uhi.pdf)
- Wu, W., Yue, S., Zhou, X., Guo, M., Wang, J., Ren, L., Yuan, B., 2020, Observational Study on the Impact of Large-Scale Photovoltaic Development in Deserts on Local Air Temperature and Humidity, *Sustainability*, 12(3403), doi: 10.3390/su12083403
- Xu, M., Bruehlisauer, M., Berger, M., 2017, Development of a new urban heat island modeling tool: Kent Vale case study Paper presented at *International Conference on Computational Science (ICCS 2017)*, Zurich, Switzerland, doi: 10.1016/j.procs.2017.05.282
- Yılmaz, E., 2015, Landsat Görüntüleri ile Adana Yüzey Isı Adası, *Cografî Bilimler Dergisi (Ankara University)*, 13(2), 115-138. doi: 10.1501/Cogbil\_0000000167
- 2014, Reducing Urban Heat Islands: Compendium of Strategies, *US Environmental Protection Agency (US EPA)*, <https://www.epa.gov/sites/production/files/2014-06/documents/basiccompendium.pdf>